Recent advances in the development of phase-shifting liquid crystal interferometers for visible and near-IR applications

Kenneth L. Marshall,*[a] Brett Klehn,[a] Bryan Watson,[a] and DeVon W. Griffin[b]
[a]Laboratory for Laser Energetics, University of Rochester
250 East River Road, Rochester, NY 14623-1299
[b]NASA Glenn Research Center, Microgravity Fluid Physics Branch, M/S 110-3
21000 Brookpark Road, Brookpark, OH 44135

ABSTRACT

Conventional phase-shifting interferometers are extremely sensitive to mechanical shock and transmitted vibration because they utilize separate test and reference optical paths that must be aligned to within a fraction of the wavelength of the light being used. Such interferometers are difficult and time consuming to set up, align, and maintain, and are costly due to the number of optics required for the dual-path design. Common-path interferometers such as the point-diffraction type are much less sensitive to environmental disturbances but until recently have not been capable of phase-shifting. The liquid crystal point diffraction interferometer (LCPDI), first demonstrated by Mercer and Creath,[1] employs a dye-doped, electro-optical LC device as the point-diffraction source to lend phase-shifting capability to the PDI common-path design. The advantage of this approach is that it combines the strengths of both types of interferometer to produce a phase-shifting diagnostic device that is much more compact, robust, and accurate than dual-path interferometers while at the same time using fewer optical elements. Such attributes make this device of special interest for diagnostic applications in the scientific, commercial, military, and industrial sectors where vibration insensitivity, power requirements, size, weight, and cost are critical issues.

In this paper, we will describe some recent activities in the areas of materials development, device design, and fabrication techniques for the original LCPDI to improve its accuracy, extend its operation to both the visible and near-IR regions of the spectrum, and to improve its temporal data collection capabilities to near video frame rates.

Key words: Liquid crystal, point diffraction, interferometry, phase shifting

1. INTRODUCTION

Conventional phase-shifting interferometers that utilize separate test and reference paths represent the most-accurate and effective way to measure changes in optical path, but their large size and extreme sensitivity to mechanical shock, vibration, temperature fluctuations, and air turbulence greatly limit their scope for potential sensing and monitoring applications. Phase-shifting interferometers function by changing the optical path difference (OPD) between the two paths of the interferometer in discrete steps that are equal fractions of a wavelength. When the unchanged wavefront from the reference path is combined with the wavefront that has passed through the test section, the differences in optical path produce interference fringes. In the conventional Mach–Zehnder and Twyman–Green designs, the OPD is changed by using a piezoelectric actuator attached to the back of the reference mirror to physically move the mirror from a central position in a sinusoidal fashion. This motion changes the OPD and thus the appearance of the resulting interferogram fringes. The changes in the position of the fringes are imaged by a detector (e.g, a CCD camera) and stored either in computer memory or on a hard storage medium such as a disk or videotape. The optical path is determined using the intensity at each pixel as a function of phase step. To obtain stable fringes, the alignment of both the test and reference paths must be maintained

*kmar@lle.rochester.edu; phone 1 585 275-8247; fax 1 585 275-5960

to within a fraction of the wavelength of the light being used for the measurement. Otherwise, the fringes will shift and may disappear. The extreme sensitivity of these interferometers to bumping, jarring, and transmitted vibration means that they must be operated on optical isolation tables in a relatively stable environment to ensure that accurate and reliable interferometric data are obtained.

Both shearing interferometers and point-diffraction interferometers (PDI), in which the test and reference beams traverse a common path, are much less vibration sensitive than the traditional interferometers described above. In these devices, the reference beam is typically generated from the test beam following the test section. Shearing interferometery suffers from a low sensitivity to high-order phase errors, low spatial resolution, and an inability to perform gradient measurements in more than two directions. In the PDI, light passing through the test section is focused onto a small diffracting object that is typically either a circle of material on a high-quality, semi-transparent glass plate or a small sphere in a glass cell (Fig. 1). The size of the focused spot is several times larger than the object so that light not intercepted by the diffracting object forms the test beam, while the diffracted light generates a perfect reference beam. The PDI has the advantages of being substantially more compact and mechanically robust than conventional phase-shifting interferometers, but suffers from the inability to use inherently more accurate phase-shifting methods[2,3] because (1) it is composed entirely of *passive* optical materials, and (2) because it is difficult to phase shift only one of two beams that traverse a common path.

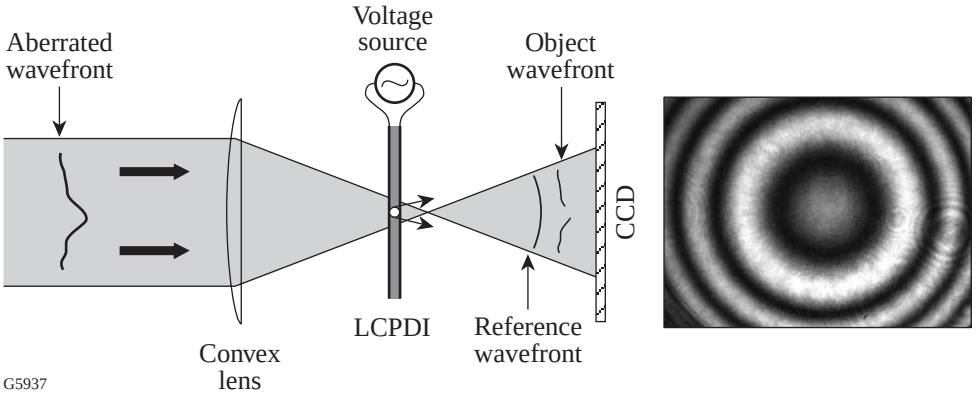

Figure 1: Schematic diagram of the LCPDI. The laser beam is focused onto an area of the liquid crystal electro-optic device containing a glass or plastic sphere in the LC fluid gap. The portion of the beam passing through the microsphere functions as the reference arm of the interferometer. Application of an electric field to the birefringent LC material produces controlled molecular reorientation with subsequent generation of interference fringes. Interference fringes obtained from a typical LCPDI device.

Mercer and Creath first demonstrated the feasibility of adding phase-shifting capability to the PDI by employing a *liquid crystal electro-optical device* as the primary modulation element.[1] They replaced the point-diffraction source and the passive, semitransparent filter of the conventional design with a liquid crystal cell containing microspheres embedded in nematic liquid crystal (LC) material (Fig. 1). The incident beam is focused on the area of the LC cell that contains an isolated microsphere, and optical interference occurs between the portions of the beam that pass through the microsphere (the reference beam) and the liquid crystal fluid. Because the area of the beam that passes through the LC fluid (the test beam) is substantially larger than the microsphere, the portion of the beam that passes through the LC fluid "host" must be attenuated using a dye as an optically absorbing "guest" in order to obtain sufficient contrast for analysis of output images. Phase shifting is accomplished by applying an ac voltage to the LC device, which induces molecular reorientation and produces a change in birefringence as a function of the magnitude of the applied voltage.

Because both the object and reference beams follow the same path, the LCPDI is relatively insensitive to the mechanical vibrations, temperature fluctuations, and air turbulence that plague conventional phase-shifting interferometers. Mercer, Creath,[4] and Rashidnia[5] first demonstrated the superior stability and robustness of the LCPDI in comparing its performance to that of a phase-shifting Mach-Zehnder interferometer. In later work, Guardalben *et al.*[6] compared the performance of an

LCPDI to that of a Zygo Mark IVxp Fizeau phase-shifting interferometer and found that the two techniques yielded measurements on the same witness sample that were in remarkably close agreement.

The LCPDI's compact size (<1 in. × 1 in.), near-solid-state robustness, and low-voltage/power requirements (1.5 V_{rms} and microamps, respectively) have led to it being described as an "interferometer on a chip," with the potential of offering comparable performance to commercial phase-shifting interferometers *at a fraction of their size, complexity, and cost.* Additional attributes of the LCPDI include the capability to collect data at *video frame rates* (with the appropriate LC material) and at a wide variety of wavelengths. The latter attribute is dependent on (1) the transparency limits of the LC material, microsphere, substrates; and (2) the availability of wavelength-specific dyes that are sufficiently soluble in the LC material to provide adequate attenuation. This combination of unique attributes makes the LCPDI of special interest for diagnostic applications in the commercial, military, scientific, and industrial sectors where physical size, robustness, rapid data collection, and low cost are of primary concern.

In this paper, we will overview two immediate areas of application for the LCPDI and describe some of our most recent activities in the areas of materials development, device design, and fabrication techniques to improve fringe contrast, to extend its operation to both the visible and near-IR regions of the spectrum, and to improve its temporal data collection capabilities to video frame rates.

2. IMMEDIATE APPLICATION AREAS AND DEVICE DEVELOPMENT GOALS

In early 2000, a four-year collaborative research effort was initiated between the University of Rochester's Laboratory for Laser Energetics (LLE) and NASA's Glenn Research Center (GRC) to study the key materials and device issues for developing the LCPDI device into a reliable and useful tool for use in microgravity fluid physics research at NASA and as a beamline diagnostic for the 60-beam, 40-TW, 1054-nm OMEGA laser system used in the Department of Energy's (DOE's) inertial confinement fusion (ICF) research at LLE. The goal of the research is to develop materials systems and fabrication methods that would lead to highly precise LCPDI devices of consistent quality for both DOE and NASA research efforts, with the long-term goal leading to devices that could be manufactured in a cost-effective manner for other applications in the scientific, commercial, military, and industrial sectors. In this section we briefly describe these applications and their requirements.

Difficulties in manufacturing of large-aperture optical elements used in the OMEGA system add aberrations to each laser beam that can result in wavefront errors in the incident beams. Such wavefront errors can manifest themselves in unequal illumination of the target, which in turn reduces the uniformity of the energy being delivered by the laser. Although numerous diagnostic instruments are used on OMEGA to analyze problems with beam uniformity, a more-effective method than is currently available is required to measure wavefront aberrations at 1054 nm. Shearing interferometery is currently used to analyze OMEGA beamlines, but the method suffers from (1) an inability to perform gradient measurements in more than two directions, (2) a low sensitivity to high-order phase errors, and (3) low spatial resolution. The large physical size and the need for vibration isolation make conventional near-IR phase-shifting interferometers impractical for these characterization activities since each of the 60 beams would have to be propagated a long distance across free space in order to reach the interferometer table. The LCPDI would solve the problem since its small size, light weight, and vibration insensitivity would allow it to be moved from beamline to beamline as needed.

To further NASA's mission of space exploration, fluid management and fundamental science in microgravity remain an active area of research. Current research topics include such diverse areas as thermocapillary flow,[7,8] nucleate boiling,[9] and diffusion of miscible fluids.[10] Future work may include the onset of turbulence and instabilities such as Marangoni–Benard and Raleigh–Taylor. All of these systems generally need to visualize or measure the mixing or temperature response of transparent liquids. Visible-region interferometry at 543 nm is the technique of choice for many such measurements. In terrestrial-based experiments where size, weight, and power are not critical issues, the use of conventional phase-shifting

interferometers mounted on large vibration isolation tables is not a barrier. But for extraterrestrial experiments in orbit, such as Dhir's proposal[9] to use holographic interferometry to study nucleate boiling in the reduced gravity environment of the International Space Station, severe volume, power, and upmass constraints along with the lack of vibration isolation suggest phase-shifting, common-path interferometry using the LCPDI as the most attractive and viable solution. In thermocapillary flow studies in enclosed chambers, the LCPDI's potential to capture interferometric data at video frame rates along with its small size would make tomographic measurements on turbulent phenomena possible—an experiment that to date has only been accomplished by using the lower-resolution Hartmann–Shack wavefront sensors.[11]

3. LCPDI DEVELOPMENT CHALLENGES

For the LCPDI to make the transition from a proof-of-concept prototype to an interferometric diagnostic of value to a wide range of users in diverse applications, substantial development work will be required. Some shortcomings of the device from our experience and from research reported by others include excessive noise in the fringes, a substantial reduction in contrast with applied voltage, speckle produced by electrohydrodynamic effects in the dye-doped liquid crystal material, device-to-device inconsistency in performance due to fabrication methodology, and (for microgravity fluid physics experiments) the inability to collect data at video frame rates. Many of these difficulties have been identified as associated with the following key areas:

3.1 LC guest–host dyes

An attenuating dye "guest" must be added to the LC "host" in order to balance the intensity of the test and reference beams to maximize fringe contrast due to the substantial difference in diameter of the two beams. The dye must satisfy a fairly stringent list of requirements to be useful in the LCPDI, including (1) a high solubility in the LC host matrix; (2) good long-term chemical, thermal, and optical stability; (3) low impact on LC order parameter; (4) large molar absorptivity; (5) low conductivity; (6) a λ_{max} at the wavelength of interest; and (7) a small or nonexistent dichroism in its absorbance with applied voltage. Poor solubility will result in low absorbance and poor fringe contrast. Excessive conductivity imparted to the LC host by the dye will produce random speckle from the mobility of charge carriers. If the dye has a large dichroic ratio (i.e., its absorbance is a function of molecular orientation), there will be large changes in fringe contrast as the applied voltage is changed. For applications in the near-IR region (e.g., 1054 nm), the issue becomes even more complicated in that only a handful of dyes are available that both absorb in the near IR *and* meet the other desired criteria.

3.2 Device fabrication

Coating defects, extrinsic particle contamination either on the microspheres or in the LC material, and entrained air bubbles in the device all can produce spatial noise in the fringe data. Devices must be assembled under Class 10 clean-room conditions and strict observance of clean-room protocol (including microfiltration of LC guest–host fluids and coating materials and scrupulous cleaning of substrates and microspheres) are paramount in the fabrication of high-quality, defect-free devices. The existing fabrication technique requires the microspheres to be placed on the substrates by hand using a high-power microscope. The microspheres are held in place only by surface static charges and can easily become dislocated and scratch the LC alignment layer when the second substrate is placed unless exceptional care is taken during cell assembly. As such, the process is highly labor intensive with the yield and quality of the devices greatly dependent on the skill of the assembler.

3.3 Response time

While the temporal response of current LCPDI devices (around 3 Hz) is adequate for applications such as beamline characterization on OMEGA where the object to be studied is in a steady-state condition, the lack of sufficient temporal response in current LCPDI devices severely limits the utility of existing LCPDI devices as a diagnostic tool for the study of transient phenomena, which comprises a major portion of fluid physics investigations. For these investigations, the device must be capable of operating at video frame rates (30 kHz), which requires a substantial improvement in temporal response over current devices.

4. LIQUID CRYSTAL MATERIALS AND DYES

The LC material used to construct the LCPDI devices is Merck E7, a commercial room-temperature nematic LC mixture of cyanobiphenyl and cyanoterphenyl compounds with a relatively high birefringence, positive dielectric anisotropy, and a broad nematic phase range. The requirement for equal intensity in both the test and reference beams of the LCPDI dictates the addition of a dye or mixture of dyes to the LC host material. The primary requirements for dyes to be suitable for the LCPDI are that they need to absorb at the wavelength of interest, have a large molar extinction coefficient to maximize attenuation efficiency [an optical density (OD) of between 1.8 and 2.5 for the test portion of the beam is necessary], and possess good solubility characteristics in the LC host to prevent long-term phase separation. For nearly all commercially available dyes that possess sufficient solubility in LC hosts, a relatively high concentration of dye (~1.5 to 2 wt%, depending on its molar extinction coefficient) is required to achieve the required O.D. values. High absorption efficiency allows thinner cells to be constructed, which allows the benefits of (1) sharper fringes and higher contrast due to improved molecular order in the LC material, (2) faster phase shifting since the electro-optical response time of the LC is a function of the square of the cell thickness, and (3) reduced risk of long-term dye precipitation. Typically, the LCPDI cell gap spacing ranges from a minimum of 8 to 10 μm to a maximum of around 20 to 25 μm, with resulting response times of 100 to 500 ms.

Elevated LC host electrical conductivity due to dye impurities (or in some cases, the chemical structure of the dye molecules) becomes a significant problem at higher dye concentrations. Many of the available commercial dyes are relatively impure and are frequently composed of a mixture of different compounds with similar chemical structures. In some cases, the precise chemical structure of the dyes is either not well defined or unknown.

Previous LCPDI devices employed dyes with a large absorption dichroism and showed voltage-dependent fringe contrast, which greatly complicated the analysis of phase-shifting data.[1,4–6] Because the largest market for dyes in LC applications is in information display where a *large* (and mainly positive) dichroic ratio is desirable, it becomes very difficult to find a suitable visible region dye that will satisfy all of the above-mentioned properties *and have no appreciable dichroism*. Although hundreds of dyes exist that have sufficient solubility in the LC host, they all exhibit some degree of dichroism as a function of their molecular structures. Design and synthesis of a dye with an extremely small or nonexistent dichroism is not beyond the realm of possibility, but the task would be very expensive, time consuming, and labor intensive. As an alternative, we investigated the concept of blending individual dyes with positive or negative dichroism in appropriate ratios into the LC host to compensate for changes in absorption with applied voltage. Table 1 shows the absorbance as a function of applied voltage for such a "compensated" mixture in a 15-μm-thick test cell.

Table 1: Change in optical density as a function of voltage for a 15- m-path-length cell containing a 2% dye mixture in E7 (8:2 ratio of negative dichroic anthraquinone dyes to positive dichroic Oil Red O dye).

Voltage (V)	Optical Density
0	1.5336
1	1.5328
2	1.5291
3	1.5294
5	1.4480
10	1.4376

The mixture contained one positive dichroic dye (Oil Red O) and five anthraquinone-based negative dichroic dyes synthesized in our laboratory in a ratio of 2:8 (positive to negative dichroic dyes). The five negative dichroic dyes were used in equal proportions to make up the negative dichroic portion of the mixture, and the total dye concentration in the Merck E7 LC host was 2% w/w. Figure 2 shows the molecular structure of these two types of dyes.

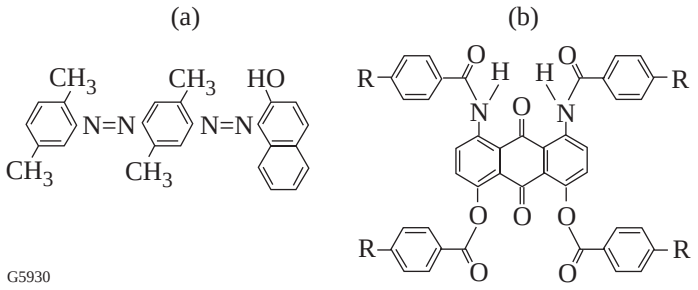

Figure 2: The molecular structures of dichroic dyes used in the "compensated" dye-doped mixture for the LCPDI (a) Oil Red O, a positive dichroic dye; (b) the generic structure for the anthraquinone dyes with negative dichroism. The "R" groups range from C_5 to C_9.

For the near-IR region of the spectrum, the selection of potential dye candidates for an LCPDI intended to operate near 1054 nm is severely limited to a total of around 10 to 20 materials. Most of these dyes used in laser applications (e.g., *Q*-switching) are ionic or highly polar and show very poor solubility in liquid crystal hosts (0.01 to 0.05 wt.%). The low solubility of these dyes in LC hosts limits their maximum blocking efficiency to an O.D. of <0.1 at a path length of 25 μm—*two decades less than required to produce acceptable fringe contrast for diagnostic purposes.*

We addressed this issue by synthesizing a series of zerovalent transition metal dithiolene complexes, which from our previous work[12,13] and the work of others,[14,15] (1) were known to have strong absorption bands in the 600- to 1500-nm region, (2) were highly soluble in liquid crystal hosts, and (3) could be designed to possess liquid crystalline properties if appropriate terminal functional groups are selected. The latter is a distinct advantage in that it would allow higher concentrations of the dye to be added to the liquid crystalline host without substantially reducing its order parameter (degree of order). Our investigations focused on compounds using nickel as the central transition element with thioalkyl termnial substituents (Fig. 3). Figure 4 shows the electro-optical behavior of a mixture of nine of these dyes in Merck E7. This new series of dyes shows a small degree of *negative* dichroism, whereas the materials synthesized previously showed only *positive* dichroism. The mixture easily exceeds the required O.D. of 2 in the off-state at a 10-μm path length. Further compensation of the dichoism is possible with the addition of existing positive dichroic nickel dithiolenes.

5. FABRICATION OF AN LCPDI

Many of the assembly techniques and materials used to fabricate LCPDI devices are well developed and are identical to those used to fabricate commercial LC devices (e.g., information displays, shutters, choppers, tunable wave plates, and spatial light modulators). Figure 5 shows a cross-sectional view of an LCPDI device. The glass substrates, typically 30 mm × 25 mm × 3-mm thick, are coated on the inner surfaces with a 200-Å layer of indium-tin oxide (ITO) conductive coating, which is itself overcoated with a 200- to 500-Å layer of a polymer alignment coating such as Nylon 6/6 or a polyimide that has been applied by spin deposition. The polymer alignment coating is buffed with a velvet roller to produce a preferred orientation direction for the LC molecules when the cell is filled. Polymer microspheres are used as reference diffraction elements and as cell spacers. The microspheres used as reference diffraction elements are placed by hand in a widely

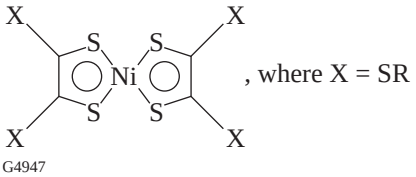

Figure 3: The molecular structure of highly soluble zerovalent nickel dithiolene dyes for near-IR LCPDI devices. The "X" groups are thioalkyl substituents with varying chain lengths and substitution positions.

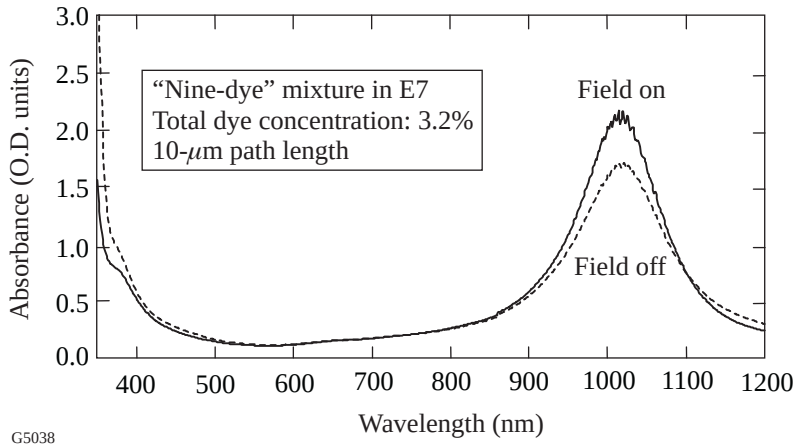

Figure 4: The electro-optical performance of a mixture of nickel dithiolene dyes in Merck E7 liquid crystal. The required O.D. of 2 is easily achieved at a 10-μm path length. The dye-doped mixture displays a small amount of negative dichroism (the absorbance increases when the electric field is applied).

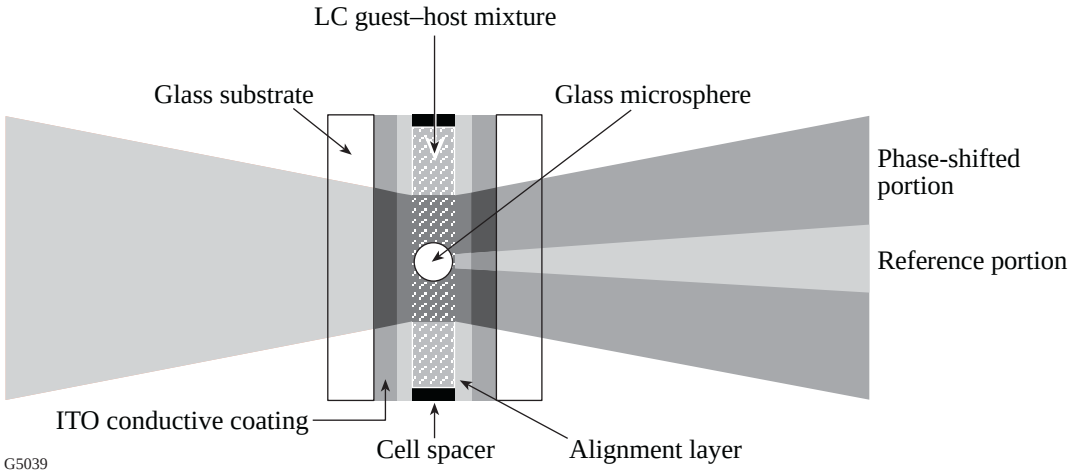

Figure 5: A cross-sectional diagram of an LCPDI cell. With a few exceptions, the fabrication techniques and materials used are the same as those used in the assembly of LC wave plates, shutters, choppers, spatial light modulators, and information displays.

separated, diamond-shaped pattern near the center of the clear aperture of the cell with the aid of a high–power optical microscope, while those used as cell spacers are dispersed into a UV-curing adhesive and applied to the coated surface near the four corners of the substrates. The substrates are carefully joined together using a specially designed fixture, and the UV adhesive is irradiated to bond the substrates. Upon successful completion of the bonding process, the cell is filled by capillary action with the dye-doped LC mixture and is edge sealed with the same UV curing adhesive.

Any defects in the coatings, extrinsic particle contamination, or air bubbles in the vicinity of the diffractive reference elements will produce spatial noise in the fringe data, as will defects or abrasions in the alignment coating produced by motion of the reference microspheres during the assembly process. To obtain high-quality, defect-free devices, all processes must be done in a Class 100 clean-room environment, with final assembly done under Class 10 conditions. Liquid crystal guest–host fluids and coating materials must be microfiltered to 0.2 μm, and both substrates and microspheres must undergo a rigorous cleaning process to eliminate foreign contaminants. Bonding of wire leads to the LCPDI device using a conductive epoxy formulation completes the assembly process. A completed LCPDI device is shown in Fig. 6.

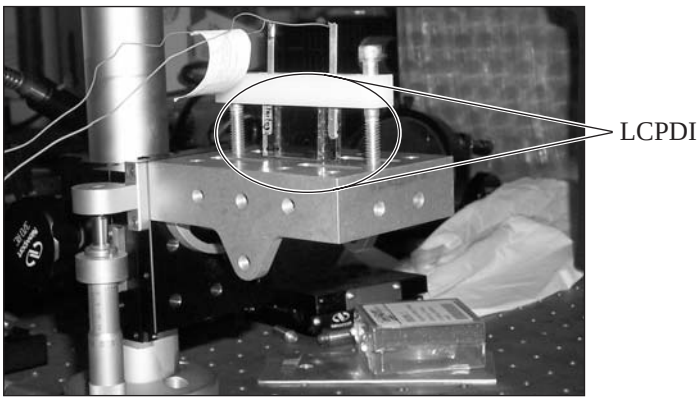

G5931

Figure 6: A completed LCPDI device, mounted in a positioning stage and ready for evaluation.

The composition of the reference diffractive microspheres plays a very important role in the ultimate performance of the LCPDI. The microspheres must be somewhat compressible in order to (1) ensure that there is intimate contact between the substrates and the sphere so as to exclude LC material, and (2) provide sufficient area to produce adequate reference beam energy for maximum fringe contrast. Glass microspheres were evaluated early on because they are available in well-defined size distributions and are chemically inert; however, we found their incompressibility to be a major problem for device fabrication. If the assembly pressure on the substrates was too low, (1) the sphere was displaced from the cell during filling with LC fluid (in the most extreme case), or (2) a small quantity of LC fluid became trapped in the contact area between the microsphere wall and the substrate. The latter situation greatly degrades contrast. Too high of an assembly pressure caused the glass microspheres to shatter. Unfortunately, the margin of error between these two extremes is quite small in practice. *Polymeric* microspheres proved to be a much better alternative for LCPDI device fabrication due to their much higher compressibility, which allows for a larger and more intimate contact area between the microsphere wall and the substrate. The result is better intensity matching between the sample and reference areas of the LCPDI and substantially improved fringe contrast. Figure 7 compares the fringe contrast of a 20-μm glass microsphere and a 24-μm polystyrene/divinyl benzene (PS/DVB) plastic sphere contained in the same 20-μm-thick LCPDI cell.

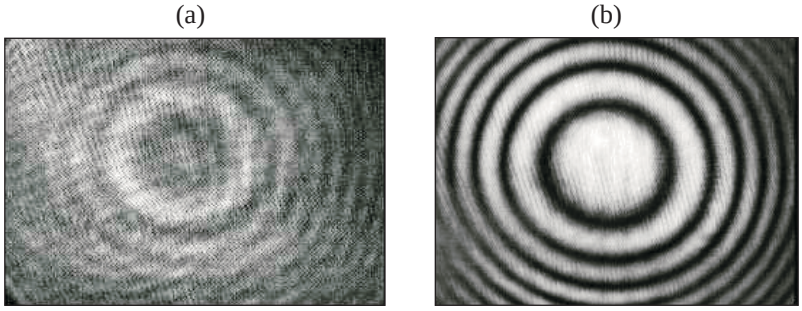

G5234

Figure 7: Comparison of interference fringes obtained from (a) a 20-μm glass microsphere and (b) a 24-μm polystyrene/divinyl benzene microsphere in the same 20-μm-thick LCPDI cell.

Figure 8 is a schematic representation of the situation. The cross-sectional area of contact between the sphere and substrate walls that is available as the reference portion of the beam (shown as the shaded areas) is substantially larger for the plastic microsphere than for the glass microsphere due to its greater compressibility, accounting in large part for the improved fringe contrast seen in Fig. 7. Our most recent experiments indicate that the best results are obtained when the diameter of the polymer reference microspheres is 1.5× larger than the intended cell gap. Additonal contributions to the improved fringe contrast come from the higher refractive index of the PS/DVB microspheres, which is a better match to the extraordinary refractive index (n_e) of the LC material.

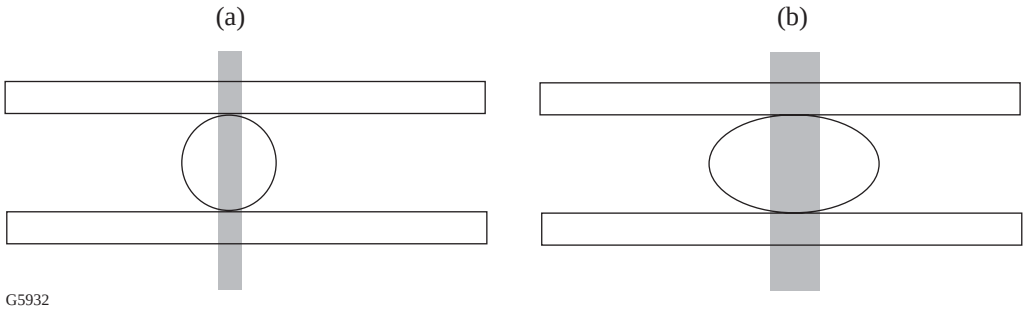

Figure 8: Schematic diagram of the compressibility of (a) the 20-μm glass microsphere and (b) the 24-μm PS/DVD microsphere in the 20-μm-thick LCPDI cell shown in Fig. 7.

One issue of initial concern was that compression of the polymer microspheres might produce stress-induced birefringence that would compromise performance of the LCPDI. Our experiments have shown that although stress-induced birefringence is produced in the microspheres during the assembly process, it appears to have little or no effect on either the fringe quality or the phase-shifting capability of the LCPDI. Figure 9 shows photomicrographs of two polymer microspheres [PS/DVD and polymethylmethacrylate (PMMA)] in two separate LCPDI devices assembled in the same manner and viewed under a polarizing microscope (100×, nearly crossed polarizers). The uniaxial isogyre in the PS/DVB microsphere is evidence of stress birefringence, which is absent in the PMMA sphere under conditions of nearly identical compression. Figure 10 compares interference fringe patterns from both devices at several applied voltage levels. The PS/DVB microspheres proved to be the diffractive element of choice for the LCPDI because (1) they are available in a wider range of diameters with narrower size distributions than are PMMA spheres, and (2) PMMA spheres are more brittle and show cracks after exposure to the LC fluid under compressive conditions over extended periods of time (weeks to months).

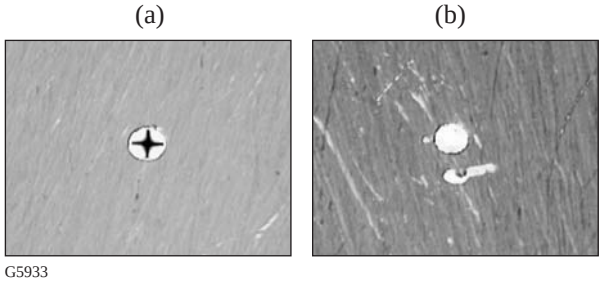

Figure 9: Photomicrographs under crossed polarizers of (a) a 42-μm-diam PS/DVD sphere and (b) a 30-μm-diam PMMA sphere each in a separate 20-μm-thick LCPDI device. The diameter of the PS/DVB sphere is ~50 μm, while the diameter of the PMMA sphere is ~40 μm. The stress birefringence due to compression in the PS/DVD sphere is quite evident.

6. ELECTRO-OPTICAL PROPERTIES AND PHASE-SHIFTING BEHAVIOR

The phase-shifting capability and its dependence on applied ac voltage was determined in a visible-region LCPDI device using a Soleil compensator inserted into the beamline of the LCPDI test-bench setup. A polarized HeNe laser and a PIN photodiode with a rotatable analyzer were used as the light source and detector, respectively. A series of fixed ac voltage levels generated by a Stanford Research Systems Model DS345, 30-MHz synthesized function generator were applied to the LCPDI device, and the amount of the electrically induced phase shift was determined by adjusting the Soleil compensator to achieve an optical minimum on the detector. Figure 11 shows curves for calculated and normalized phase-shift data plotted on a common axis as a function of voltage for a 22-μm-thick LCPDI device. The response curve over the full voltage range is highly nonlinear, as is expected due to the quadratic nature of the response of the LC material to the ac field; however, because small increments of applied voltage produce substantial phase shifts, it is easily possible to find sections of the response curve in which to operate where the phase shift with applied voltage is linear and predictable.

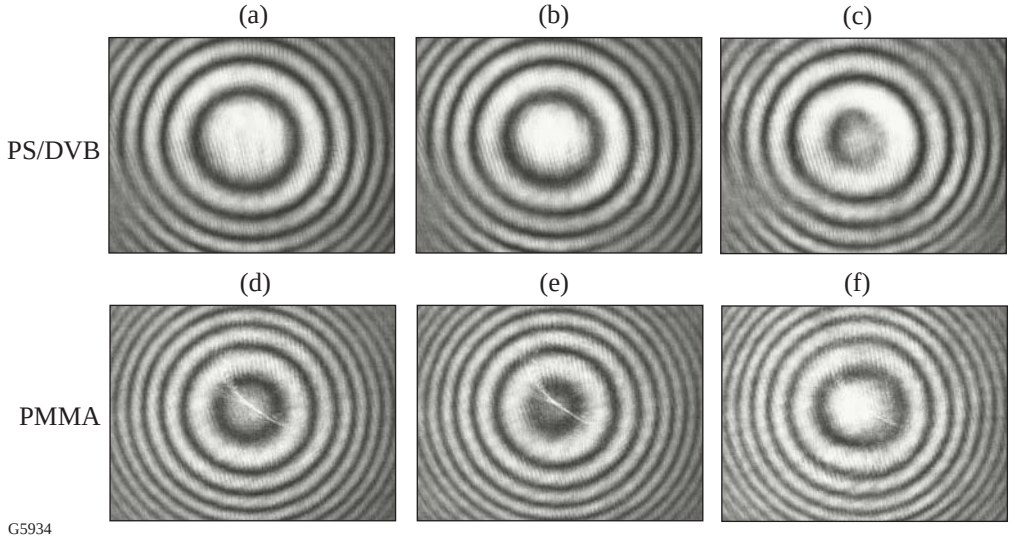

Figure 10: Voltage-controlled fringe shifting for two separate LCPDI devices containing PS/DVB and PMMA reference microspheres, respectively. PS/DVB (a,b,c) and PMMA (d,e,f) at 1.0 V (a and d), 1.25 V (b and e) and 1.37 V (c and f).

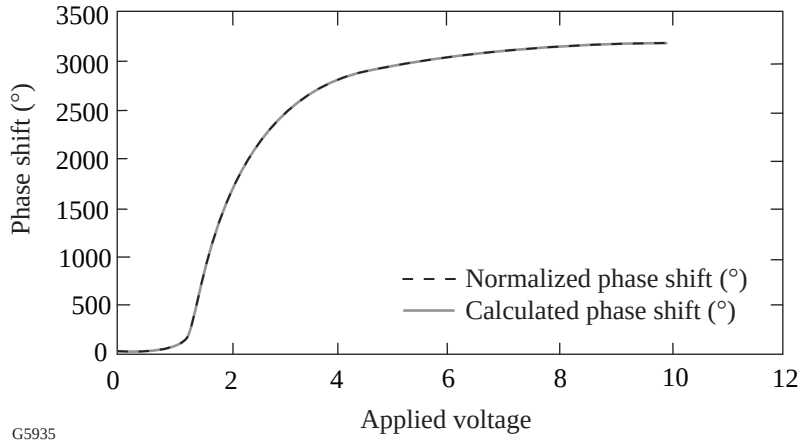

Figure 11: Phase shift data as a function of voltage for a 22-μm-thick LCPDI device. Although the magnitude of the electrically induced phase shift is highly nonlinear over the entire voltage range, its efficiency per unit voltage is so large that only small sections of the total curve need to be used to achieve linear and predictable phase shifting.

With the relationship between applied voltage and phase shift established, the response time between any two levels of phase shift can be determined by evaluating the change in dielectric constant (determined as a capacitance change) of the LC guest–host mixture as a function of applied voltage. Since the perceived dielectric constant and the index of refraction in LC materials are both related mathematically to the orientation of the LC molecules with respect to the applied electric (or optical) field, changes in molecular orientation will have an identical effect on both the birefringence and the cell impedance. Changes in cell impedance with time immediately after application of discrete voltage levels can be directly correlated with the temporal phase-shift response under the same conditions. The advantage of this approach is that the measurement technique is relatively simple and rapid, requires no laser source or optical components, and can ultimately be used as a feedback-control mechanism to precisely control optic axis orientation (and thus phase shift) through custom driving waveforms.

Changes in impedance as a function of time were determined by measuring the voltage across a resistor connected in series with the LCPDI cell. The typical impedance value of the series resistor was around 100 Ω, which is insignificant compared to 100-kΩ impedance of the LCPDI cell. Because the SRS digital function generator was unable to switch between two voltage-state levels without going through an intermediate zero-voltage state approaching 100 ms, the output of two identical SRS function generators, preset to voltage values V_1 and V_2, was fed into a custom-built circuit consisting of an analog demultiplexer with a switch that allowed the output of the test circuit to switch between V_1 and V_2 with a delay of only 4 ns. The circuit also contains a dip-switch–selectable series resistor and a variable-gain operational amplifier for the series resistor. Voltage changes across the series resistor with time were amplified and imaged on an Hewlett Packard 54520A digital oscilloscope to produce a plot of current versus time (since the current is determined solely by the impedance of the cell). This current increase follows the equation of a first-order exponential shown as the voltage across the test resistor as given by:

$$V(t) = V_{peak} - a * e^{(-bt)}.$$

Selecting two points along the curve as *a* and *b* and inputting these values along with the voltage levels into the above equation gives a mathematical model for the envelope of the signal. Using this model, the rise times to go from the initial phase-shift value to either 95% or 99% of the final phase-shift value can be calculated free from noise. Tables 2 and 3 give response time data at several voltage levels for a 360° phase shift in 10-μm- and 22-μm-thick LCPDI cells, respectively. Response times for both rising voltages [$V_2 > V_1$ (t_{rise})] and falling voltages [$V_2 < V_1$ (t_{decay})] are reported in the tables.

Table 2: Response time data for a 0∞to 360∞phase shift in a 10- m-path LCPDI device.

V_1	V_2	t_{rise} (seconds)	Frequency ($1/t_{rise}$)	t_{decay} (seconds)	Frequency ($1/t_{decay}$)
2.13	3.16	0.1200	8.06	0.28	3.57
2.52	8.00	0.0170	58.82	0.17	5.88
2.69	10.00	0.0076	131.58	0.15	6.67
Note: Rise time and decay time were measured from initial value to 99% of steady state.					

Table 3: Response time data for a 0∞to 360∞phase shift in a 22- m LCPDI cell.

V_1	V_2	t_{rise} (seconds)	Frequency ($1/t_{rise}$)	t_{decay} (seconds)	Frequency ($1/t_{decay}$)
1.50	1.73	>2.20	<0.45	>2.36	<0.42
2.20	3.00	1.08	0.93	1.44	0.69
4.50	10.00	0.04	25.00	0.12	8.33
Note: Rise time and decay time were measured from initial value to 99% of steady state.					

7. SUMMARY AND FUTURE DEVELOPMENTS

Although substantial progress has been made toward improving the fringe contrast, reproducibility, and data collection capabilities of the LCPDI in its current form, a number of technical hurdles still remain to be overcome before the LCPDI can be considered as a robust device that could be widely used by non-optics professionals. Additional visible region dye candidates with larger molar extinction coefficients need to be identified and/or developed in order to allow construction

of devices with the thinnest possible path length to optimize both fringe contrast and response time. Electrical conductivity imparted to the host by addition of the dyes (both visible and near IR) is a persistent problem that will also limit the minimum achievable cell thickness without competition from electrohydrodynamic effects. For the near-IR region, our plan to address this issue is to prepare zerovalent dithiolene dyes using palladium as the central metal. These materials are known to have a conductivity about one order of magnitude lower than the corresponding nickel complexes, but are much more difficult to prepare.

For the LCPDI to evolve past the level of a laboratory prototype, radical changes need to be made to the current "hand-fabrication" process in order to achieve the robustness, uniformity, and device-to-device performance consistency required for it to be widely accepted as a useful diagnostic tool. We are investigating a new fabrication technique for the "next-generation" LCPDI device that makes the reference diffracting elements and spacers an *integral part of the substrates* through deposition of a suitable optical material directly on the substrate surface. These "structured" substrates would eliminate many of the assembly difficulties and performance limitations of the current LCPDI device as well as open the possibility *of mass-producing LCPDI devices at low cost by the same processes used to manufacture commercial LC displays.* Deposition approaches under consideration include vapor-deposited inorganic thin films, photolithographic patterning of a spin-deposited photosensitive polymer, and contact printing of a thermoplastic, thermosetting, or UV-cured optical polymer onto the substrate surface. Some promising preliminary work has already been done in this area.

This development in turn opens a new challenge of how to apply and process an LC alignment layer on the structured substrate in a manner that does not physically damage or compromise the structural elements. Although the classical mechanical buffing technique has been used successfully in the past to fabricate hundreds of LC circular polarizers and wave plates containing Ta_2O_5 spacer elements for the OMEGA laser system, we anticipate that the much smaller aspect ratio of the LCPDI diffractive central elements as compared to these spacers puts them at much greater risk of either damage or complete removal by the mechanical shear forces present during the buffing action. We are instead investigating the use of new LC alignment coatings in which the preferred LC alignment direction is generated *photochemically* using polarized UV light. The advantages of this approach are as follows: (1) it is non-contacting and thus mechanically non-destructive with respect to the structured substrates; (2) unlike buffing, no extraneous particles are generated; and (3) the equipment and process are compatible with Class 10 clean-room conditions.

Achieving further reductions in response time will require additional effort in two areas: (1) driving waveforms and electronics, and (2) LC materials. Efforts are underway to develop custom driving waveforms, electronics, and software to maximize control over the phase-shifting capability and provide a user friendly interface for setting up and conducting characterization activities. In the materials area, we are looking at the possibility of using dual-frequency-addressed nematic LC materials to provide bi-directional field-driven control over the LC optic axis (most nematic LC materials rely on field-free relaxation to return to their original orientation) and *ferroelectric* LC materials. The latter materials are of special interest because their response time can be up to two orders of magnitude faster than nematic LC materials, and because the optic axis orientation is field driven in both directions, depending on the applied field polarity. Another advantage is that the electro-optic response for the ferroelectric LC's is inherently field linear and displays no threshold effect. The more highly ordered and layered structure of these LC materials, however, will pose some special new challenges in terms of ordering around discontinuous surfaces (such as the reference diffraction elements in the LCPDI), molecular alignment, and device fabrication.

Although a substantial amount of development work remains to be done before the LCPDI can be considered a "standard" characterization tool for interferometry, this "interferometer on a chip" has a bright future as a phase-shifting diagnostic device for applications in the scientific, commercial, military, and industrial sectors where vibration insensitivity, power requirements, size, weight, and cost are critical issues. Further research in the key areas of materials development, hardware/software control, and device fabrication will yield LCPDI devices that are highly accurate, physically robust, and able to be manufactured at low cost using commercial LCD manufacturing technology.

ACKNOWLEDGMENT

This work is supported by the U.S. Department of Energy Office of Inertial Confinement Fusion under Cooperative Agreement No. DE-FC03-92SF19460 and the University of Rochester. The support of DOE does not constitute an endorsement by DOE of the views expressed in this article. This work was also supported by the NASA Glenn Research Center, Cleveland, OH, under NASA grant # NAG3-2348.

REFERENCES

1. C. R. Mercer and K. Creath, "Liquid-crystal point-diffraction interferometer," *Opt. Lett.* **19**(12), 916–918 (1994).
2. P. Hariharan, B. F. Oreb, and N. Brown, "Real-time holographic interferometry: A microcomputer system for the measurement of vector displacements," *Appl. Opt.* **22**(6), 876–880 (1983).
3. K. Creath, "Phase-measurement interferometry techniques," in *Progress in Optics XXVI*, edited by E. Wolf, Chap. V, pp. 349–383, North-Holland, Amsterdam, 1988.
4. C. R. Mercer and K. Creath, "Liquid-crystal point-diffraction interferometer for wave-front measurements," *Appl. Opt.* **35**(10), 1633–1642 (1996).
5. C. R. Mercer, N. Rashidnia, and K. Creath, "High data density temperature measurement for quasi steady-state flows," *Exp. Fluids* **21**(1), 11–16 (1996).
6. M. J. Guardalben, L. Ning, N. Jain, D. J. Battaglia, and K. L. Marshall, "Experimental comparison of a liquid-crystal point-diffraction interferometer (LCPDI) and a commercial phase-shifting interferometer and methods to improve LCPDI accuracy," *Appl. Opt.* **41**(7), 1353–1365 (2002).
7. M. Kassemi and N. Rashidnia, "Dynamics of oscillatory thermocapillary and natural convection in free surface problems," presented at the 37th Aerospace Sciences Meeting and Exhibit, Reno, NV, 11–14 January 1999 (AIAA paper 99-0704).
8. M. Kassemi and N. Rashidnia, "Steady and oscillatory flows generated by a bubble in 1-G and low-G environments," presented at the 35th Aerospace Sciences Meeting and Exhbit, Reno, NV, 6–9 January 1997 (AIAA paper 97-0924).
9. D. M. Qiu, V. K. Dhir, D. Chao, M. M. Hasan, E. Neumann, G. Yee, and A. Birchenough, "Single-bubble dynamics during pool boiling under low gravity conditions," *J. Thermophys. Heat Transf.* **16**(3), 336–345 (2002).
10. N. Rashidnia, R. Balasubramaniam, J. Kuang, P. Petijeans, and T. Maxworthy, "Measurement of the diffusion coefficient of miscible fluids using both interferometry and Wiener's method," *Int. J. Thermophys.* **22**(2), 547–555 (2001).
11. L. McMackin, R. J. Hugo, R. E. Pierson, and C. R. Truman, "High speed optical tomography system for imaging dynamic transparent media," *Opt. Express* **1**(11), 302–311 (1997).
12. K. L. Marshall and S. D. Jacobs, "Near-infrared dichroism of a mesogenic transition metal complex and its solubility in nematic hosts," *Mol. Cryst. Liq. Cryst.* **159**, 181–196 (1988).
13. "Design and synthesis of near-infrared absorbing dyes for the liquid crystal point-diffraction interferometer (LCPDI)," Laboratory for Laser Energetics *LLE Review* **81**, 37–47, NTIS document No. DOE/SF/19460-335 (1999). Copies may be obtained from the National Technical Information Service, Springfield, VA 22161.
14. U. T. Mueller-Westerhoff, A. Nazzal, R. J. Cox, and A. M. Giroud, "Mesomorphic transition metal complexes. IV. Dithiene complexes of Ni, Pd, and Pt," *Mol. Cryst. Liq. Cryst. Lett.* **56**(8), 249–255 (1980).
15. K. Ohta, A. Takagi, H. Muroki, I. Yamamoto, K. Matsuzaki, T. Inabe, and Y. Maruyama, "Discotic liquid crystals of transition metal complexes. IV. Novel discotic liquid crystals obtained from substituted bis(dithiolene)nickel complexes by a new method," *Mol. Cryst. Liq. Cryst.* **147**, 15–24 (1987).